

# The light-quark mass dependence of the nucleon axial charge

F. Alvarado and L. Alvarez-Ruso

*Instituto de Física Corpuscular (IFIC) and Departamento de Física Teórica,  
Consejo Superior de Investigaciones Científicas (CSIC) and  
Universidad de Valencia (UV), E-46980 Paterna, Valencia, Spain.*

Received 13 January 2022; accepted 23 February 2022

The light-quark mass dependence of the nucleon axial isovector charge ( $g_A$ ) has been analysed up to NNLO,  $\mathcal{O}(p^4)$ , in relativistic chiral perturbation theory using extended-on-mass-shell renormalization, without and with explicit  $\Delta(1232)$  degrees of freedom. In the  $\Delta$ -less case at this order, the  $g_A(M_\pi)$  dependence of lattice QCD simulations cannot be reproduced using low energy constants extracted from pion-nucleon phenomenology. A good description of these LQCD data is only accomplished in the theory with  $\Delta$ . From this fit we obtain  $g_A(M_{\pi(\text{phys})}) = 1.260 \pm 0.012$  close to the experimental results and  $d_{16} = -0.88 \pm 0.88 \text{ GeV}^{-2}$  in agreement with  $\pi N \rightarrow \pi\pi N$ . The sizeable errors are of theoretical origin, reflecting the difference between  $\mathcal{O}(p^3)$  and  $\mathcal{O}(p^4)$  at large  $M_\pi$ .

*Keywords:* Light-quark; NNLO.

DOI: <https://doi.org/10.31349/SuplRevMexFis.3.0308095>

## 1. The axial charge in baryon ChPT

The axial isovector charge  $g_A$  is a fundamental property of the nucleon, associated to the difference in the spin fractions carried by  $u$  and  $d$  quarks. The matrix element of the axial isovector current  $A_\mu^\alpha(x) = \bar{q}(x) (\gamma_\mu \gamma_5 \tau^\alpha / 2) q(x)$ , with  $q = (u, d)^T$  the quark doublet, taken between nucleon states, can be written as

$$\begin{aligned} \langle N(p') | A_\mu^\alpha(0) | N(p) \rangle &= \bar{u}(p') \\ &\times \left[ \gamma_\mu F_A(q^2) + \frac{q_\mu}{2m_N} F_P(q^2) \right] \gamma_5 \frac{\tau^\alpha}{2} u(p), \end{aligned} \quad (1)$$

where  $\tau^a$  are the Pauli matrices and  $q = p' - p$  is the momentum transferred to the nucleon;  $p^2 = p'^2 = m_N^2$ .  $F_A(q^2)$  and  $F_P(q^2)$  are the nucleon axial and induced pseudoscalar form factors. The axial charge is nothing but  $g_A \equiv F_A(q^2 = 0)$ . Accurately extracted from neutron  $\beta$  decay (see Ref. [1] for a recent determination),  $g_A$  is a benchmark for lattice QCD (LQCD) studies [2].

Chiral perturbation theory (ChPT) is the effective theory of QCD at low energies. It allows to determine the light ( $u, d$ ) quark mass dependence of hadronic observables in terms of low-energy constants (LECs) and perform model-independent extrapolations of LQCD to the physical point. ChPT can also account for finite volume and lattice spacing corrections in a systematic way [3, 4]. Moreover, it has proved helpful to deal with the contamination from excited states [5–7]. The synergy between ChPT and LQCD can also be used to determine LECs which are difficult to access experimentally. This is the case of  $d_{16}$ , present in the  $\mathcal{O}(p^3)$  part of the  $\pi N$  Lagrangian. This parameter has been regarded as one of the most important sources of uncertainty in the quark mass dependence of nuclear properties such as ground-state and binding energies [8–10]. On the other hand, this LEC dictates the slope of the light-quark mass (or, equivalently,

pion-mass,  $M_\pi$ ) dependence of  $g_A$  close to the chiral limit. Therefore, it is natural to extract it from LQCD at low pion masses (see [11] and references therein).

In order to describe the  $M_\pi$  dependence of  $g_A$  and extract  $d_{16}$ , we have calculated the axial charge in relativistic baryon ChPT (BChPT) up to NNLO with explicit  $\Delta$ . We use the extended-on-mass-shell (EOMS) renormalization scheme [12], so that not only the power counting, but also the analytic properties of the loops are preserved.

Up to NNLO  $\equiv \mathcal{O}(p^4) \equiv \mathcal{O}(M_\pi^3)$  with explicit  $\Delta$ ,  $g_A$  can be cast as

$$\begin{aligned} g_A &= \mathring{g}_A + 4d_{16}M_\pi^2 + g_{A(\text{loop})}^{(3)\Delta}(\mathring{g}_A; M_\pi) \\ &+ g_{A(\text{loop})}^{(3)\Delta}(\mathring{g}_A, h_A, g_1; M_\pi) \\ &+ g_{A(\text{loop})}^{(4)\Delta}(\mathring{g}_A, c_1, c_2, c_3, c_4; M_\pi) \\ &+ g_{A(\text{loop})}^{(4)\Delta}(\mathring{g}_A, h_A, g_1, c_1, a_1, b_4, b_5; M_\pi). \end{aligned} \quad (2)$$

Details about the relevant terms in the Lagrangian, Feynman diagrams and renormalization can be found in Ref. [11].

## 2. Pion mass dependence of the axial coupling using LECs from $\pi N$ scattering

Before extracting the LECs from LQCD, we investigate how well do the LECs extracted from experiments describe  $g_A(M_\pi)$ . In Ref. [13], elastic  $\pi N$  and inelastic  $\pi N \rightarrow \pi\pi N$  scattering have been studied up to  $\mathcal{O}(p^4)$  in covariant ChPT using a modified version of the EOMS approach [14]. The  $c_{1-4}$  LECs that enter  $g_A(M_\pi)$  at  $\mathcal{O}(p^4)$  in the  $\Delta$ -less model were extracted, together with  $d_{16}$ , owing to the inclusion of  $\pi N \rightarrow \pi\pi N$  in the combined analysis. We have converted these LECs from their modified EOMS to the conventional one (details in Ref. [11]). The chiral limit axial coupling,  $\mathring{g}_A$ , is determined from  $g_A(M_\pi = M_{\pi(\text{phys})} = 135 \text{ MeV})$ ,

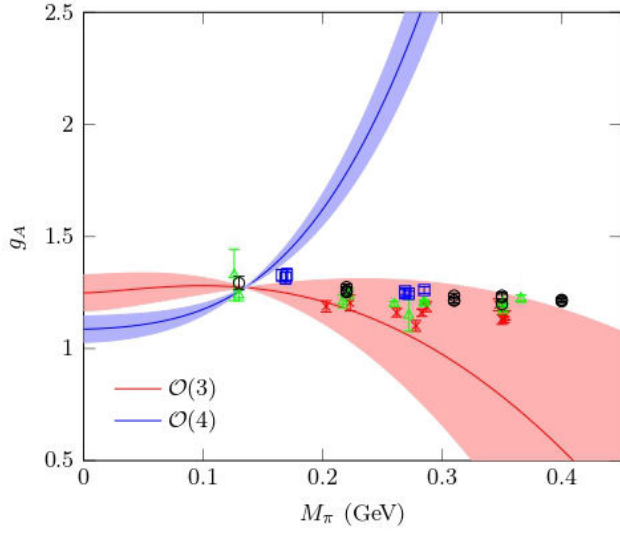


FIGURE 1.  $g_A(M_\pi)$  at  $\mathcal{O}(p^3)$  (red) and  $\mathcal{O}(p^4)$  (blue) using phenomenological input from Ref. [13]. The LQCD data from CalLat 18 [15] (black circles), Mainz 19 [16] (red crosses), RQCD 19 [7] (green triangles) and NME 21 [17] (blue squares) are shown at finite  $a$  values, without (small) discretization corrections.

TABLE I.  $\hat{g}_A$  and  $d_{16}$  used to predict  $g_A(M_\pi)$  in the  $\Delta$  model.

	$\mathcal{O}(p^3)$	$\mathcal{O}(p^4)$
$\hat{g}_A$	$1.251 \pm 0.051$	$1.089 \pm 0.030$
$d_{16} (\text{GeV}^{-2})$	$-2.2 \pm 1.1$	$-1.86 \pm 0.80$

$\hat{g}_A, d_{16}, c_i = g_{A(\text{phys})} = 1.2754(13)_{\text{exp}}(2)_{\text{RC}}$  [1]. The values for  $d_{16}$  and  $\hat{g}_A$  are given in Table I while  $c_{1-4}$  are the same as in the second column of Table II. Up to higher orders, the pion decay constant and the nucleon mass in the chiral limit are  $F_\pi \simeq F_{\pi(\text{phys})} = 92.2$  MeV and  $\hat{m} \simeq m_{N(\text{phys})} + 4c_1 M_\pi^2(\text{phys})$ , with  $m_{N(\text{phys})} = 939$  MeV.

The obtained  $g_A(M_\pi)$  at  $\mathcal{O}(p^3)$  and  $\mathcal{O}(p^4)$  are shown in Fig. 1 together with recent LQCD determinations.  $1\sigma$  error bands from the LECs' uncertainties are depicted. We assume Gaussian-distributed errors. Correlations are neglected since the uncertainty is clearly dominated by the  $d_{16}$  error.

The  $\mathcal{O}(p^3)$  agrees with the lattice determinations, although the tension increases with  $M_\pi$ . On the contrary, it is clear that the  $\mathcal{O}(p^4)$  prediction does not describe the  $M_\pi$  dependence of LQCD data. We have checked that alternative  $c_{1-4}$  determinations [18, 19] do not reduce the disagreement. This conflict between the light-quark mass dependence of  $g_A$  at  $\mathcal{O}(p^4)$  and phenomenology was already noted in non-relativistic heavy-baryon (HB) ChPT [20, 21], and we have shown that it is also present in the relativistic version of the theory. This disagreement at  $\mathcal{O}(p^4)$  could be caused by an accidental slow convergence of  $g_A$  in BChPT. On the other hand, adding degrees of freedom (*dofs*) such as the  $\Delta$  [21] resonance might solve the problem. Some of the additional LECs needed to obtain  $g_A(M_\pi)$  with explicit  $\Delta$  have not been phenomenologically determined, so that we do not give

any prediction in this model. We do study  $g_A$  with explicit  $\Delta$  in our own fits to LQCD in the next Sec. 3.

### 3. Analysis of LQCD data and LEC determination

#### 3.1. Data set and fit strategy

Recent developments, in particular about excited-state contamination, have led to LQCD results that agree with the  $g_A$  experimental value at the level of a few percent [2]. Therefore, we only have in our data set results with an improved treatment of these effects. We analyse renormalized  $\{g_A^i\}$  data at different  $\{M_\pi^i, a_i\}$  values, where  $a$  stands for the lattice spacing, from CalLat 18 [15], Mainz 19 [16], RQCD 19 [7] (with  $m_s \sim m_{s(\text{phys})}$ ) and NME 21 [17] (fit  $\{4^{N_\pi}, 3^*\}$  averaged over  $Z_1$  and  $Z_2$  renormalizations). We only consider large lattices ( $M_\pi L \geq 3.5$ ), for which we can neglect finite volume effects.

In order to evaluate the performance of BChPT at  $\mathcal{O}(p^3)$  and  $\mathcal{O}(p^4)$  for  $g_A(M_\pi)$ , and to extract  $\hat{g}_A$  and  $d_{16}$  LECs, we perform fits to the ensemble of LQCD results introduced above. For this purpose we define

$$\chi^2 = \sum_i \frac{(g_A(M_\pi^i, a_i) - g_A^i)^2}{(\Delta g_A^i)^2} + \chi_{\text{prior}}^2. \quad (3)$$

Additionally, we account for discretization corrections as  $g_A(M_\pi^i, a_i) = g_A(M_\pi^i) + x_j a_i^{n_j}$ , where  $x_j$  are free parameters, with  $j = 1, 2, 3, 4$  for  $\{\text{CalLat 18, Mainz 19, RQCD 19, NME 21}\}$ , respectively, and the  $n_{1,4} = 1, n_{2,3} = 2$  are action specific. Let us stress that these corrections are small and do not change the extracted LECs, although they reduce the  $\chi^2/\text{dof}$ .

In order to improve the description of the data and reduce correlations [22], we assume naturalness for free LECs,  $\Lambda^{n-1} c_n \sim 1$ , and therefore we define:

$$\chi_{\text{prior}}^2 = \sum_{\text{free LECs}} \left( \frac{\Lambda^{n-1} c_n}{5} \right)^2; \quad (4)$$

$c_n$  denotes a LEC of  $\mathcal{O}(p^n)$  and  $\Lambda = 1 \text{ GeV} \sim 4\pi F_\pi$  [23, 24]. We anticipate that a prior for  $\hat{g}_A$  is superfluous, since it is tied to a natural value by low  $M_\pi$  data.

The large contribution of  $\mathcal{O}(p^4)$  discussed in the previous section indicates that the error associated with the truncation of the chiral series should be included. Following [25] we estimate it as:

$$|\Delta g_A^{(n+1)}| = \max \left\{ Q^{n+1} |g_A^{(0)}|, Q^n |\Delta g_A^{(1)}|, \dots, Q |\Delta g_A^{(n)}| \right\}, \quad (5)$$

where  $\Delta g_A^{(m)} = g_A^{(m)} - g_A^{(m-1)}$  encompasses all the monomials that start at order  $m$  and  $Q$  is the expansion variable, which in this case is  $Q = M_\pi/\Lambda$ . Notice that in our  $\mathcal{O}(p^3)$

fits we deliberately do not assume any information about  $\mathcal{O}(p^4)$ , and therefore the truncation error for these calculations is different than the one for the  $\mathcal{O}(p^4)$  case ([11] for details).

Altogether, in Eq. (3)  $(\Delta g_A^i)^2 = (\Delta g_{ALQCD}^i)^2 + (\Delta g_{A\chi}(M_\pi^i))^2$ . In this way, however, LQCD and truncation errors are not independent. Therefore, following Ref. [14], we plot them as two different error bands for  $g_A(M_\pi)$ . Moreover, as a measure of the agreement of our best-fit curve with the data, we also give the  $\chi_0^2$  value without truncation error:

$$\chi_0^2 = \sum_i \frac{(g_A(M_\pi^i, a_i) - g_A^i)^2}{(\Delta g_{ALQCD}^i)^2}. \quad (6)$$

We have also investigated the convergence by varying the range of  $M_\pi$  in which the fit is performed. We have seen that the  $\chi^2$  and the LECs reach a plateau when the maximum  $M_\pi$  included is between 300 and 400 MeV (see Fig. 5 of Ref. [11]). The consideration of theoretical errors allows to

extend the analysis to a broader range of  $M_\pi$  because LQCD points with large  $M_\pi$ , where the convergence is worse, have a larger combined uncertainty.

### 3.2. Fit results

The fit results for the different models are displayed in Fig. 2. Starting by the  $\mathcal{O}(p^3)$   $\Delta$ , we actually find that the description in this model is misleadingly good. Looking at the results of the  $\mathcal{O}(p^4)$   $\Delta$  fit, one can see a large contribution from  $\mathcal{O}(p^4)$  as in Sec. 2. These terms are much larger than the truncation error of the  $\mathcal{O}(p^3)$  fit, estimated from  $\mathcal{O}(p)$  and  $\mathcal{O}(p^3)$ . Therefore an  $\mathcal{O}(p^4)$  calculation is necessary to account realistically for the  $M_\pi$  dependence.

In the  $\mathcal{O}(p^4)$   $\Delta$  calculation the  $c_{1-4}$  enter the picture. We fix them to their central phenomenological values [13] in Table II (letting them vary constrained to their uncertainties yields substantially the same result). The accord of the

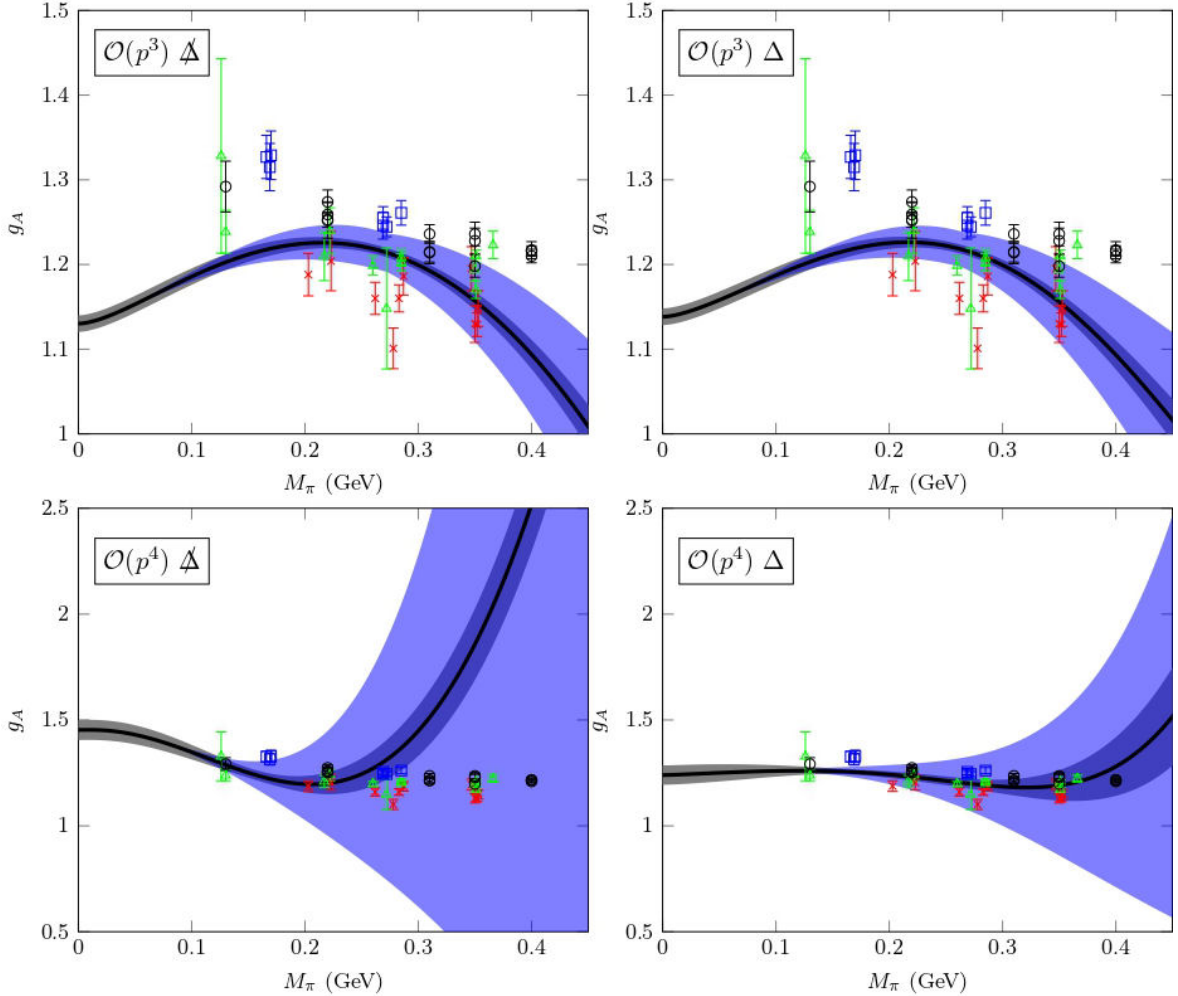


FIGURE 2.  $g_A(M_\pi)$  LQCD fits with  $\mathcal{O}(p^3)$  and  $\mathcal{O}(p^4)$  relativistic BChPT without and with  $\Delta(1232)$  as explicit *dof*. Gray (dark) bands correspond to errors determined by propagating LEC uncertainties. Blue bands represent the estimated theoretical uncertainties  $\Delta g_{A\chi}^{(4,5)}$ . The LQCD points are the same as in Fig. 1.

TABLE II. LEC values, both fixed and fitted to LQCD data, in the four different models under study.

	$\mathcal{O}(p^3) \not\Delta$	$\mathcal{O}(p^4) \not\Delta$	$\mathcal{O}(p^3) \Delta$	$\mathcal{O}(p^4) \Delta$
$\mathring{g}_A$ (free)	$1.1302 \pm 0.0098$	$1.453 \pm 0.048$	$1.1383 \pm 0.0099$	$1.240 \pm 0.046$
$d_{16}$ ( $\text{GeV}^{-2}$ ) (free)	$-0.925 \pm 0.055$	$-9.77 \pm 0.87$	$1.224 \pm 0.040$	$-0.88 \pm 0.88$
$h_A$	-	-	1.35	1.35
$g_1$	-	-	-2.29	-2.29
$c_1$ ( $\text{GeV}^{-1}$ )	-	$-0.89 \pm 0.06$	-	$-1.15 \pm 0.05$
$c_2$ ( $\text{GeV}^{-1}$ )	-	$3.38 \pm 0.15$	-	$1.57 \pm 0.10$
$c_3$ ( $\text{GeV}^{-1}$ )	-	$-4.59 \pm 0.09$	-	$-2.54 \pm 0.05$
$c_4$ ( $\text{GeV}^{-1}$ )	-	$3.31 \pm 0.13$	-	$2.61 \pm 0.10$
$a_1$ ( $\text{GeV}^{-1}$ )	-	-	-	0.90
$\tilde{b}_4$ ( $\text{GeV}^{-2}$ ) (free)	-	-	-	$-12.3 \pm 1.0$
$\mathring{m}$ (GeV)	0.874	0.874	0.855	0.855
$\mathring{m}_\Delta$ (GeV)	-	-	1.166	1.166
$\chi^2/\text{dof}$	$36.06/(43 - 6) = 0.98$	$13.31/(43 - 2) = 0.33$	$37.60/(43 - 6) = 1.02$	$11.14/(43 - 7) = 0.31$
$\chi_0^2/\text{dof}$	11.48	2995.63	11.87	13.93

$\mathcal{O}(p^4) \not\Delta$  model with the data is poor. It is reflected in the large  $\chi_0^2$  and the unnatural  $d_{16}$  value despite being constraint by a prior. It has been shown in HB ChPT [20] that agreement can be achieved by including contributions of  $\mathcal{O}(p^{5,6})$ . We have instead followed a different path, introducing the  $\Delta$  as an explicit *dof*. This option is supported in Ref. [21] based on the Adler-Weisberger sum rule and a HB ChPT  $g_A$  calculation.

In the model with  $\Delta$  we fix  $h_A$  to its large- $N_c$  value,  $h_A = 1.35$  [13], close to its phenomenological value [19]. The large- $N_c$  limit gives  $|g_1| = 2.29$  [13, 19]. We choose the negative value, suggested by  $\pi N$  elastic scattering [19] and our own analysis of the  $F_A$  (to be reported elsewhere). In addition, we fix  $\mathring{m}_\Delta \simeq m_{\Delta(\text{phys})} - 4a_1 M_{(\text{phys})}^2$  with  $m_{\Delta(\text{phys})} = 1232$  MeV and  $a_1 = 0.90$   $\text{GeV}^{-1}$  from [26].

When performing the fit up to  $\mathcal{O}(p^3)$  and comparing it with the  $\mathcal{O}(p^4)$  the situation resembles the  $\not\Delta$  case: the  $\mathcal{O}(p^4)$  fit yields  $\mathcal{O}(p^4)$  terms that are larger than the error estimated in the  $\mathcal{O}(p^3)$  one. Consequently, it is necessary to introduce the whole  $\mathcal{O}(p^4)$ .

In the light of our results, the calculation that we regard as a realistic description of  $g_A(M_\pi)$  is the  $\mathcal{O}(p^4)$  one with explicit  $\Delta$ . Here we fix the  $c_{1-4}$  to the values extracted from  $\pi N$  scattering [14], which account for the  $\Delta$  pole, in good agreement with  $\pi N + \pi\pi N$  fits [13]. In addition, we have two more LECs,  $b_4$  and  $b_5$ . These appear at  $\mathcal{O}(p^4)$  in the combination  $\tilde{b}_4 \simeq b_4 + (12/13)b_5$ . Hence, we only fit as a free parameter  $\tilde{b}_4$  and neglect the higher order monomials proportional to  $b_5$ .

The result of this fit satisfactorily describes the trend of  $g_A(M_\pi)$  predicted in the lattice up to relatively high  $M_\pi$ . The theoretical error is sizeable at high  $M_\pi$  due to the large contribution of  $\mathcal{O}(p^4)$  terms. Still, the description of LQCD

points and convergence are highly improved with respect to the  $\mathcal{O}(p^4) \not\Delta$  model. The last column of Table II displays the extracted LECs. The  $\tilde{b}_4$  seems unnatural, but one should remind that it is a combination of LECs. We have noted that correlations among LECs are large. This reflects a certain degeneracy that could be partially lifted adding an extra dimension, *i.e.* studying also the  $q^2$  dependence of the  $F_A$ . The extracted  $d_{16} = -0.88 \pm 0.88$   $\text{GeV}^{-2}$  is in good agreement with the determinations from  $\pi N \rightarrow \pi\pi N$  with explicit  $\Delta$  pole [13], which, translated to standard EOMS is  $d_{16(\text{pheno})} = -1.0 \pm 1.0$   $\text{GeV}^{-2}$ . Although the  $g_A$  is in principle the most suitable observable to extract  $d_{16}$ , the convergence issues lead to an error comparable with the phenomenological one. The  $\mathring{g}_A$  value is higher than in the  $\mathcal{O}(p^3)$  fits, leading to a  $g_A(M_{\pi(\text{phys})}) = 1.260 \pm 0.012$  close to the experimental value.

## 4. Conclusions

We have studied the  $M_\pi$  dependence of the nucleon axial coupling up to  $\mathcal{O}(p^4)$  (NNLO) in relativistic BChPT with EOMS renormalization. At this order, but without explicit  $\Delta$ , we have shown that the  $g_A$  obtained using LECs extracted from  $\pi N$  elastic and inelastic scattering does not describe the  $M_\pi$  dependence of lattice data. This feature has been earlier noticed in HB ChPT [20, 21], and persists in the relativistic theory.  $\mathcal{O}(p^4)$  terms become large already from  $M_\pi \gtrsim 200$  MeV, suggesting that  $\mathcal{O}(p^3)$  analyses of  $g_A(M_\pi)$  underestimate theoretical uncertainties.

In line with the conclusions of Ref. [21], we can satisfactorily describe the LQCD data for  $g_A(M_\pi)$  at  $\mathcal{O}(p^4)$  only after the  $\Delta$  is included as an explicit *dof*. However, although in a much smaller degree than in the  $\not\Delta$  model, a rapid increase

in the size of  $\mathcal{O}(p^4)$  terms with  $M_\pi$  is observed and reflected in the theoretical uncertainty. Together with the large correlations, which could be reduced by fitting the  $q^2$  dependence of the axial form factor, this implies that heavier resonances and/or  $\mathcal{O}(p^5)$  terms are still required to reach a good convergence and reduce theoretical uncertainties. Setting the baryon masses in the loops to the values obtained by the LQCD simulations might be also worth exploring in view of the findings of Ref. [27] although this would correspond to the resummation of baryon selfenergy insertions of higher order. For this

purpose it would be convenient to have more input about the  $\Delta$  pole position for the different lattice ensembles.

From our  $\mathcal{O}(p^4)$  fit we have obtained  $g_A(M_{\pi(\text{phys})}) = 1.260 \pm 0.012$  close to the experimental result and  $d_{16} = -0.88 \pm 0.88 \text{ GeV}^{-2}$  in good agreement with  $\pi N$  phenomenology. As a consequence of the aforementioned issues, errors are still sizeable for  $d_{16}$ . Our ongoing work to extend the study to the whole axial form factor (at low  $q^2$ ) may provide more information about  $d_{16}$ , as well as other LECs such as  $d_{22}$ .

- 
1. Mikhail Gorchtein and Chien-Yeah Seng. Dispersion relation analysis of the radiative corrections to  $g_A$  in the neutron  $\beta$ -decay. *JHEP*, **10** (2021) 053.
  2. Y. Aoki *et al.*, *FLAG Review* **2021** (2021) 11.
  3. Silas R. Beane and Martin J. Savage. Nucleon properties at finite lattice spacing in chiral perturbation theory. *Phys. Rev. D* **68** (2003) 114502.
  4. Silas R. Beane and Martin J. Savage. Baryon axial charge in a finite volume. *Phys. Rev. D* **70** (2004) 074029.
  5. Brian C. Tiburzi. Time Dependence of Nucleon Correlation Functions in Chiral Perturbation Theory. *Phys. Rev. D* **80** (2009) 014002.
  6. Oliver Bar. Chiral perturbation theory and nucleon-pionstate contaminations in lattice QCD. *Int. J. Mod. Phys. A*, **32** (2017) 1730011.
  7. G. S. Bali *et al.*, Nucleon axial structure from lattice QCD. *JHEP*, **05** (2020) 126.
  8. S. R. Beane and Martin J. Savage. The Quark mass dependence of two nucleon systems. *Nucl. Phys. A*, **717** (2003) 91.
  9. J. C. Berengut *et al.*, Varying the light quark mass: impact on the nuclear force and Big Bang nucleosynthesis. *Phys. Rev. D*, **87** (2013) 085018.
  10. E. Epelbaum, Hermann Krebs, Timo A. Lähde, Dean Lee, and Ulf-G. Meißner. Dependence of the triple-alpha process on the fundamental constants of nature. *Eur. Phys. J. A* **49** (2013) 82.
  11. F. Alvarado and L. Alvarez-Ruso, The light-quark mass dependence of the nucleon axial charge and pion-nucleon scattering phenomenology. arXiv, 2112.14076, (2021).
  12. T. Fuchs, J. Gegelia, G. Japaridze, and S. Scherer, Renormalization of relativistic baryon chiral perturbation theory and power counting. *Phys. Rev. D* **68** (2003) 056005.
  13. D. Siemens *et al.*, Elastic and inelastic pionnucleon scattering to fourth order in chiral perturbation theory. *Phys. Rev. C* **96** (2017) 055205.
  14. D. Siemens *et al.*, Elastic pion-nucleon scattering in chiral perturbation theory: A fresh look. *Phys. Rev. C* **94** (2016) 014620.
  15. C. C. Chang *et al.*, A per-cent-level determination of the nucleon axial coupling from quantum chromodynamics. *Nature*, **558** (2018) 91.
  16. Tim Harris *et al.*, Nucleon isovector charges and twist-2 matrix elements with  $N_f = 2 + 1$  dynamical Wilson quarks. *Phys. Rev. D* **100** (2019) 034513.
  17. S. Park *et al.*, Precision Nucleon Charges and Form Factors Using 2+1-flavor Lattice QCD. *arXiv* **2103** (2021) 05599.
  18. Yun-Hua Chen, De-Liang Yao, and H. Q. Zheng, Analyses of pion-nucleon elastic scattering amplitudes up to  $\mathcal{O}(p^4)$  in extended-on-mass-shell subtraction scheme. *Phys. Rev. D*, **87** (2013) 054019.
  19. De-Liang Yao *et al.*, Pionnucleon scattering in covariant baryon chiral perturbation theory with explicit Delta resonances. *JHEP*, **05** (2016) 038.
  20. V. Bernard and Ulf-G. Meißner, The Nucleon axialvector coupling beyond one loop. *Phys. Lett. B* **639** (2006) 278.
  21. M. Procura, B. U. Musch, T. R. Hemmert, and W. Weise, Chiral extrapolation of  $g(A)$  with explicit Delta(1232) degrees of freedom. *Phys. Rev. D*, **75** (2007) 014503.
  22. S. Wesolowski, N. Klco, R. J. Furnstahl, D. R. Phillips, and A. Thapaliya, Bayesian parameter estimation for effective field theories. *J. Phys. G* **43** (2016) 074001.
  23. A. Manohar and H. Georgi, Chiral Quarks and the Nonrelativistic Quark Model. *Nucl. Phys. B* **234** (1984) 189.
  24. S. Scherer and M. R. Schindler, *A Primer for Chiral Perturbation Theory*, volume **830** (2012).
  25. E. Epelbaum, H. Krebs, and U. G. Meißner. Improved chiral nucleon-nucleon potential up to next-to-next-to-next-to-leading order. *Eur. Phys. J. A*, **51** (2015) 53.
  26. L. Alvarez-Ruso, T. Ledwig, J. Martin Camalich, and M. J. Vicente-Vacas, Nucleon mass and pion-nucleon sigma term from a chiral analysis of lattice QCD data. *Phys. Rev. D*, **88** (2013) 054507.
  27. Matthias F. M. Lutz, Ulrich Sauerwein, and Rob G. E. Timmermans, On the axial-vector form factor of the nucleon and chiral symmetry. *Eur. Phys. J. C*, **80** (2020) 844.